

https://doi.org/10.1070/QEL18064

Dynamics of three-photon laser excitation of mesoscopic ensembles of cold rubidium atoms to Rydberg states

D.B. Tretyakov, V.M. Entin, E.A. Yakshina, I.I. Beterov, I.I. Ryabtsev

Abstract. **The temporal dynamics of three-photon $5S_{1/2} \rightarrow 5P_{3/2} \rightarrow 6S_{1/2} \rightarrow 39P_{3/2}$ laser excitation of mesoscopic ensembles of cold Rb atoms to Rydberg states in a magneto-optical trap is studied using cw single-frequency lasers at each stage. The ensembles comprise $N = 1-5$ atoms and are detected by the method of selective field ionisation with postselection with respect to the number of atoms. The dependence of the excitation probability on the duration of the exciting laser pulses and the number of detected Rydberg atoms is investigated. At short interaction times, a linear increase in probabilities is observed, and at large times, the probabilities reach saturation, while each number of atoms has its own characteristic features. The experimental dependences are compared with the results of numerical calculations in the framework of a four-level model, and their good agreement is obtained. The conditions necessary for observing Rabi population oscillations are determined. The obtained results are important for the application of Rydberg atoms in quantum information.**

Keywords: *Rydberg atoms, three-photon excitation, spectroscopy, dynamics, detection statistics, laser cooling.*

1. Introduction

Laser excitation of atoms to Rydberg states with principal quantum numbers $n \gg 1$ is used to implement quantum calculations and simulations with qubits based on single atoms in arrays of optical dipole traps [1–3]. Atoms in Rydberg states interact with each other much stronger than atoms in the ground or low-excited states, because the dipole moments of atoms increase as n^2 [4]. Quantum entangled states of two atoms, which are the basis of two-qubit operations, arise due to the dipole blockade effect, when the excitation of one Rydberg atom blocks the excitation of neighbouring atoms [5, 6]. Upon laser excitation of Rydberg atoms, it is also possible to implement quantum simulations in mesoscopic ensembles of atoms [7].

As qubits based on neutral atoms, hydrogen-like atoms of alkali metals Rb and Cs, in which the wavelengths of optical transitions fall within the operating range of high-efficiency semiconductor and solid-state lasers, are mainly used [3]. For Rb atoms, as a rule, a two-stage excitation scheme $5S \rightarrow 5P \rightarrow nS$, nD with a wavelength of 780 nm in the first stage and 480 nm in the second stage is used [8, 9]. The use of counter-propagating laser beams partially suppresses the residual Doppler effect, which arises due to the finite temperature of atoms in optical traps and leads to a loss of coherence [10].

Three-photon laser excitation scheme is interesting because it can provide excitation of cold Rydberg atoms free of recoil and Doppler effects, thereby eliminating the heating of atoms upon absorption of photons and providing a higher fidelity of quantum operations with Rydberg atoms. In our earlier theoretical paper [11], we showed that for this excitation to be implemented, it is necessary to fulfill the condition that the sum of the wave vectors of the exciting laser radiations be equal to zero for the star-shaped geometry of three beams. We have not yet implemented this idea, because it requires a special magneto-optical trap with a specific configuration of the optical windows of its vacuum chamber. However, previously [12–14] we experimentally studied the three-photon $5S_{1/2} \rightarrow 5P_{3/2} \rightarrow 6S_{1/2} \rightarrow nP$ excitation spectra of cold Rb Rydberg atoms in an operating magneto-optical trap using cw single-frequency lasers at each stage and detecting single Rydberg atoms by the method of selective field ionisation (SFI) [4].

In Ref. [12], we observed two partially overlapping peaks with different amplitudes in the spectra of three-photon $5S_{1/2} \rightarrow 5P_{3/2} \rightarrow 6S_{1/2} \rightarrow nP$ laser excitation at small frequency detunings of laser radiation from intermediate single-photon resonances. These peaks corresponded to coherent three-photon excitation and incoherent three-step excitation due to the presence of two different excitation paths through the dressed states of the intermediate levels. In Ref. [13], only a single coherent three-photon resonance was observed in the spectra of three-photon $5S_{1/2} \rightarrow 5P_{3/2} \rightarrow 6S_{1/2} \rightarrow 37P_{3/2}$ laser excitation as frequency detunings of laser radiation were increased. For pulses shorter than 0.5 μs, an additional Fourier broadening of the spectra occurred and Rabi oscillations appeared at the wings of three-photon resonances. The spectra of three-photon $5S_{1/2} \rightarrow 5P_{3/2} \rightarrow 6S_{1/2} \rightarrow nP_{3/2}$ laser excitation were studied in Ref. [14] for random mesoscopic ensembles of $N = 1-5$ cold Rydberg Rb atoms with the principal quantum number

D.B. Tretyakov, V.M. Entin, I.I. Ryabtsev Rzhanov Institute of Semiconductor Physics, Siberian Branch, Russian Academy of Sciences, prosp. Akad. Lavrent'eva 13, 630090 Novosibirsk, Russia; e-mail: ryabtsev@isp.nsc.ru
E.A. Yakshina Rzhanov Institute of Semiconductor Physics, Siberian Branch, Russian Academy of Sciences, prosp. Akad. Lavrent'eva 13, 630090 Novosibirsk, Russia; Institute of Laser Physics, Siberian Branch, Russian Academy of Sciences, prosp. Akad. Lavrent'eva 15B, 630090 Novosibirsk, Russia;
I.I.Beterov Rzhanov Institute of Semiconductor Physics, Siberian Branch, Russian Academy of Sciences, prosp. Akad. Lavrent'eva 13, 630090 Novosibirsk, Russia; Institute of Laser Physics, Siberian Branch, Russian Academy of Sciences, prosp. Akad. Lavrent'eva 15B, 630090 Novosibirsk, Russia; Novosibirsk State Technical University, prosp. Karla Marksa 20, 630073 Novosibirsk, Russia

Received 27 March 2022
Kvantovaya Elektronika **52** (6) 513–522 (2022)
Translated by V.L. Derbov

n = 39, 81, 110 in a magneto-optical trap. We found that for an excitation volume of 15 – 20 μm in size at n = 39, the effect of dipole blockade was completely absent, while for n = 81 and 110, partial dipole blockade was observed with a decrease in the probability of excitation of more than two atoms.

The experimental implementation of a complete dipole blockade and two-qubit operations requires coherent (with Rabi population oscillations) laser excitation of single atoms to Rydberg states. In the present work, we studied the temporal dynamics of three-photon $5S_{1/2} \rightarrow 5P_{3/2} \rightarrow 6S_{1/2} \rightarrow 39P_{3/2}$ laser excitation of mesoscopic ensembles of cold Rb atoms to Rydberg states in a magneto-optical trap. Ensembles of Rydberg atoms consisted of $N = 1-5$ atoms and were detected by the SFI method with postselection by the number of atoms. The aim of this work was to study the dependence of the excitation probabilities of a certain number of atoms on the duration of the exciting laser pulses. The experimental dependences were also compared with the results of numerical calculations in the framework of a four-level theoretical model, and the conditions necessary for observing Rabi oscillations were determined.

2. Experimental setup

The experiments were performed with cold ^{85}Rb atoms trapped in a magneto-optical trap (MOT), schematically shown in Fig. 1a [2, 12–14]. Three orthogonal pairs of light waves with a wavelength of 780 nm cooled the atoms. The cooling laser was tuned to the closed transition $5S_{1/2}(F = 3) \rightarrow 5P_{3/2}(F = 4)$ of the ^{85}Rb isotope, and the repump laser was tuned to the transition $5S_{1/2}(F = 2) \rightarrow 5P_{3/2}(F = 3)$. At the centre of the trap, a cloud 0.5–1 mm in size was formed, containing approximately 10^6 cold atoms at a temperature of 100–200 μK.

Experiments on the spectroscopy of three-photon excitation were carried out in a MOT switched off for a short time

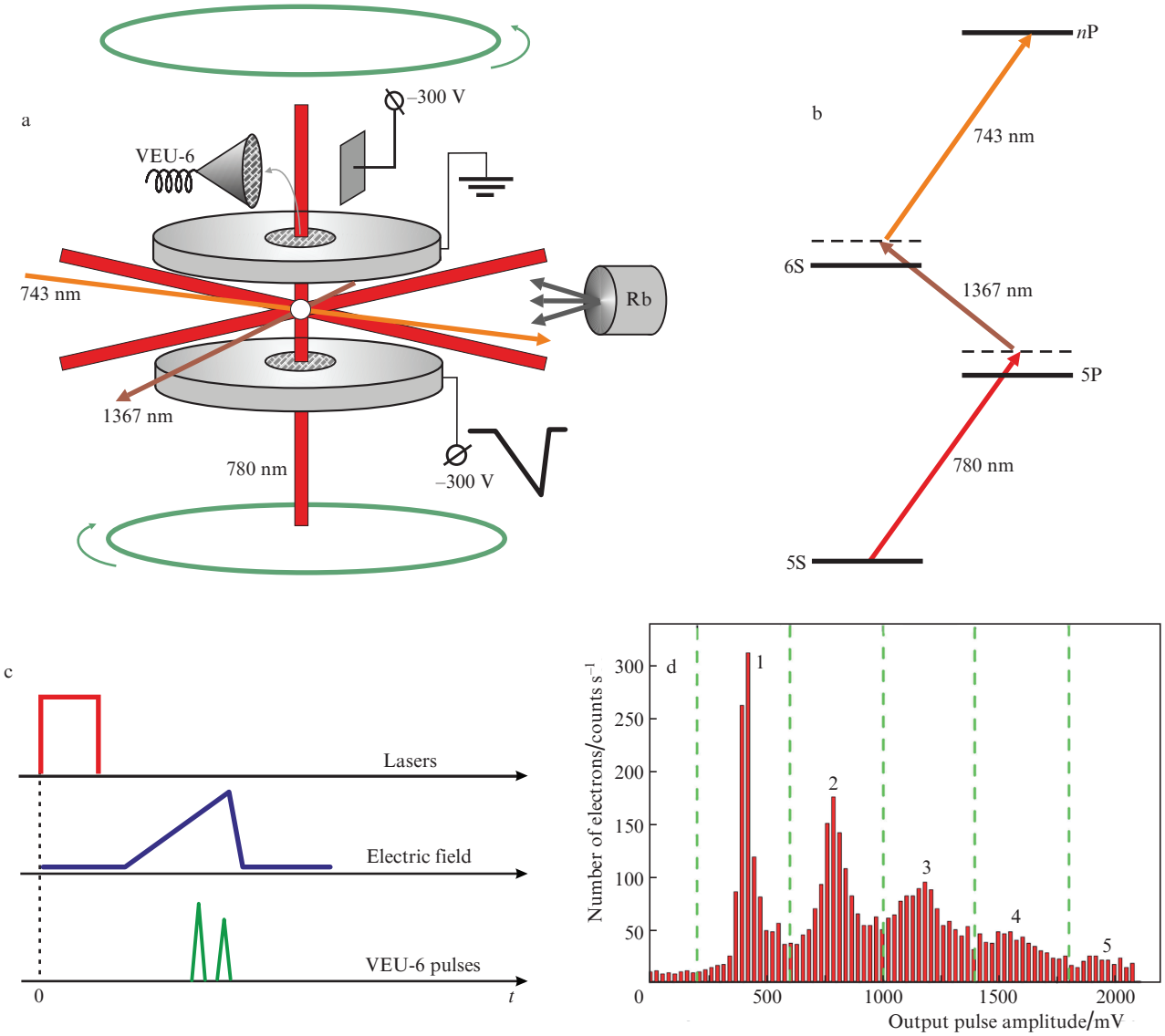

Figure 1. (Colour online) (a) Schematic of the experiment with cold Rydberg ^{85}Rb atoms in a magneto-optical trap, where the Rydberg atoms are excited in a small volume of a cloud of cold atoms and detected using the method of selective field ionisation. (b) Schematic of coherent three-photon laser excitation $5S_{1/2} \rightarrow 5P_{3/2} \rightarrow 6S_{1/2} \rightarrow nP_{3/2}$ of Rb Rydberg atoms with detuning of laser frequencies from intermediate resonances. (c) Timing diagram of laser and electric pulses. (d) Histogram of the output pulses of the secondary channel electron multiplier VEU-6, which detects electrons formed by selective field ionisation. Separate peaks are observed corresponding to $N = 1-5$ recorded Rydberg atoms.

beforehand. For this purpose, acousto-optic modulators (AOMs) were installed in all cooling laser beams, to turn them off for 20 μs, and turn them on again after the measurement. The MOT gradient magnetic field was not turned off during the measurements, but its influence was minimised by adjusting the position of the excitation volume to a point near the zero magnetic field. This adjustment was controlled by the absence of Zeeman splitting of the $37P_{3/2} \rightarrow 37S_{1/2}$ microwave transition at a frequency of 80 GHz using the method of our paper [15]. This allowed using high repetition rate of laser pulses (5 kHz) and monitoring the variation of signals from Rydberg atoms in real time on the oscilloscope screen and in the computer data acquisition system. At the same time, the presence of a non-switched-off gradient magnetic field can lead to Zeeman broadening of three-photon resonances by an additional value of $\Gamma_Z/(2\pi) \approx 0-0.5$ MHz.

The excitation of cold Rb atoms to the nP Rydberg states ($n = 30-100$) was carried out according to the three-stage scheme $5S_{1/2} \rightarrow 5P_{3/2} \rightarrow 6S_{1/2} \rightarrow nP_{3/2}$ (Fig. 1b). The first stage $5S_{1/2}(F = 3) \rightarrow 5P_{3/2}(F = 4)$ was excited by radiation from a Toptica DL PRO external-cavity diode laser with a wavelength of 780 nm, the frequency of which was stabilised by the saturated absorption resonance in the cell with the Rb atom vapour. The measured laser linewidth was $\Gamma_1/(2\pi) \approx 0.3$ MHz. The output laser radiation was passed through an AOM, which formed pulses of arbitrary duration with edges of 100 ns. The AOM also provided a blue detuning $\delta_1/(2\pi) = +80$ MHz of the radiation frequency from the exact atomic resonance to avoid the population of the $5P_{3/2}$ intermediate level.

At the second stage, $5P_{3/2}(F = 4) \rightarrow 6S_{1/2}(F = 3)$, radiation with a wavelength of 1367 nm from a cw single-frequency external-cavity diode laser (Sacher TEC150) was used. The radiation frequency of this laser is stabilised by the resonance of a high-stability optical Fabry–Perot interferometer (Stable Laser Systems ATF). The measured laser linewidth was $\Gamma_2/(2\pi) \approx 0.3$ MHz. The output laser radiation was passed through an electro-optical modulator (EOM) with a modulation depth of 20 dB, which formed pulses of arbitrary duration with 2-ns edges. The laser emission frequency also had a blue detuning $\delta_2/(2\pi) = +82$ MHz from the exact atomic resonance so as not to populate the $6S_{1/2}$ intermediate level.

At the third stage, the nP Rydberg states were excited from the $6S_{1/2}(F = 3)$ state by the radiation from a cw Ti : sapphire ring laser (Tekhnoscan TIS-SF-07). When tuning the laser radiation in the wavelength range of 738–745 nm, it is possible to selectively excite fine-structure sublevels with $J = 1/2$, 3/2 of the Rydberg nP states with principal quantum numbers $n = 30-120$. The laser radiation frequency was stabilised using the resonance of the same highly stable optical Fabry – Perot interferometer. The measured laser linewidth $\Gamma_3/(2\pi) \approx 0.01$ MHz. The AOM was installed at the output of the laser to operate in a pulsed regime with edges 100 ns long.

The laser radiation of the second and third stages was supplied to the MOT through single-mode optical fibres. At the exit from the fibres, the radiation was collimated and then focused on a cloud of cold atoms in the geometry of beams crossed at right angles (Fig. 1a) with waist diameters of 10 μm for radiation with $\lambda = 743$ nm and 20 μm for radiation with $\lambda = 1367$ nm. In the intersection region of the focused beams, an effective volume of excitation of Rydberg atoms 15–30 μm in size was formed, depending on the relative position of the waists and the presence or absence of saturation of the transitions. The laser radiation of the first stage with $\lambda = 780$ nm was not focused, had a beam diameter of 1 mm, and was directed at a cloud of cold atoms at angles of 45° towards the other beams. Atoms were excited to Rydberg states by laser pulses with a repetition rate of 5 kHz.

Atoms were excited in the space between two stainless steel plates producing a uniform electric field (Fig. 1a). The electric field was used for Stark spectroscopy and detection of Rydberg atoms by the SFI method. Rydberg atoms were detected with a repetition rate of 5 kHz when the ionising electric field sweep pulse was switched on with a rise time of 2–3 μs. The electrons formed due to ionisation were accelerated by the electric field, flew through the metal mesh of the upper plate, and were directed with the help of a deflecting electrode into the input socket of the VEU-6 channel electron multiplier. A high-speed ADC, a strobe integrator, and a computer processed pulse signals from its output. The number of electrons recorded per laser pulse was determined by the number of Rydberg atoms in the excitation region and the overall efficiency of electron detection [16]. In our experiments, the detection efficiency reached 70% [17].

The timing diagram of signals in the registration system is shown in Fig. 1c. After each laser pulse, which excited some of the cold atoms to the Rydberg state nP, the ionising electric field was swept with a rise time of about 2 μs. Depending on the state of the Rydberg atom, ionisation occurred at different times after the laser pulse. Next, a pulsed ionisation signal was recorded at the VEU-6 output using a strobe pulse corresponding in time to the ionisation of the nP state. Figure 1d shows a histogram of the amplitudes of the pulses output from the VEU-6. It shows several peaks corresponding to different numbers N of detected Rydberg atoms ($N = 1-5$).

After each laser pulse, the data acquisition system measured the amplitude of the VEU-6 output pulse, then the number of recorded atoms was determined from the pre-measured histogram (Fig. 1d). Then, after accumulating data for 10^3-10^4 laser pulses, the signals were sorted by the number N of atoms and the probability of three-photon laser excitation of the Rydberg state was calculated.

3. Theory of three-photon laser excitation

In the theoretical description, we denoted the states of the rubidium atom by the letter k: $k = 0$ for the ground state $5S_{1/2}(F = 3)$, $k = 1$ for the first intermediate state $5P_{3/2}(F = 4)$, $k = 2$ for the second intermediate state $6S_{1/2}(F = 3)$ and $k = 3$ for the Rydberg state $nP_{3/2}$ (Fig. 1b). For each intermediate single-photon transition with the number $j = 1, 2, 3$, the corresponding Rabi frequency $\Omega_j = d_j E_j/\hbar$ and detuning δ_j are introduced. Here d_j are the dipole moments of single-photon transitions, and E_j are the electric field amplitudes for linearly polarised light fields. The total detuning $\delta = \delta_1 + \delta_2 + \delta_3$ of the three-photon $0 \rightarrow 3$ transition can be scanned by scanning the frequency of any laser.

As we showed in Ref. [11], in the absence of spontaneous relaxation of all levels and at sufficiently large laser frequency detunings from intermediate resonances ($\Omega_1 \ll |\delta_1|$, $\Omega_2 \ll |\delta_2|$), the population of the Rydberg state can be calculated by solving the Schrödinger equation for the probability amplitudes a_k for each state $k = 0-3$ in the rotating wave approximation. As a result, we obtain the dependence of the population of the Rydberg state on the interaction time t for coherent three-photon laser excitation:

$$|a_3|^2 \approx \frac{\Omega^2}{\Omega^2 + (\delta + \Delta_0 + \Delta_3)^2} \times \frac{1 - \cos\left(t\sqrt{\Omega^2 + (\delta + \Delta_0 + \Delta_3)^2}\right)}{2}, \quad (1)$$

where $\Omega = \Omega_1\Omega_3\Omega_3/(4\delta_1\delta_3)$ is the effective Rabi frequency for three-photon excitation $\Delta_0 = \Omega_1^2/(4\delta_1)$ and $\Delta_3 = \Omega_3^2/(4\delta_3)$ are the light shifts of states 0 and 3, respectively. Equation (1) shows that the condition for an exact three-photon resonance is $\delta + \Delta_0 + \Delta_3 = 0$, with the population oscillating between the ground and Rydberg states at frequency Ω. Equation (1) also describes the excitation spectrum of the Rydberg state during scanning δ for a fixed interaction time t.

In a more realistic theoretical model that takes into account the spontaneous relaxation of the excited levels 1–3, the Rabi oscillations decay with a damping constant $\gamma = 1/\tau$, which is determined by the reciprocal lifetime of the Rydberg state τ, or even faster if the detunings of the intermediate resonances are not large enough. In this case, the population of the Rydberg state reaches a certain stationary value. We built such a model earlier in the four-level approximation based on the optical Bloch equations for the density matrix [12]. It is not possible to find an exact analytical solution for the population ρ_{33} of the Rydberg state at arbitrary Rabi frequencies and detunings; therefore, generally, it is necessary to solve the problem numerically. However, at weak excitation ($\Omega \ll \gamma$) and large detunings of laser radiation frequencies from intermediate resonances, our four-level system can be approximated by an effective two-level system with a direct optical transition $0 \rightarrow 3$. For this system, we have found the approximate solution:

$$\rho_{33} \approx \frac{\Omega^2}{2\Omega^2 + \gamma^2 + 4\delta^2}\left[1 + e^{-\gamma t} - 2e^{-\gamma t/2}\cos\left(t\sqrt{\Omega^2 + \delta^2}\right)\right]. \quad (2)$$

Equation (2) shows that at large interaction times ($\gamma t \gg 1$) the Rabi oscillations decay and the population reaches a stationary value described by the Lorentz contour of the excitation spectrum.

In addition, the developed theoretical model [12] makes it possible to take into account the finite widths of the emission lines Γ_i of all three lasers in the phase diffusion model, when random phase fluctuations are present in laser radiation, but there are no amplitude fluctuations [18]. In order to consider them in the equations for the density matrix for optical coherences, an imaginary part equal in absolute value to $\Gamma_i/2$ is added to each detuning δ_i to introduce additional decay in the coherences. Our numerical calculations according to this model showed good agreement between experiment and theory [12, 13]. However, it should be borne in mind that in such a model the laser radiation spectrum has a Lorentzian shape, while lasers usually have a Gaussian line profile with a faster decay at the wings. Therefore, the theoretical excitation spectra of the Rydberg states in this model may have some discrepancies with the experimental data at their wings.

4. Spectra and dynamics of three-photon laser excitation of mesoscopic ensembles of cold atoms to Rydberg states

Since our system of detecting Rydberg atoms based on selective field ionisation offers an opportunity to measure the number of atoms and implement post-selection of signals with sorting by the number of atoms, we studied the spectra and dynamics of three-photon laser excitation of mesoscopic ensembles of cold atoms to Rydberg states with the number of atoms $N = 1-5$.

The dots in Figs 2a–2f show the experimental spectra of three-photon laser excitation of the $39P_{3/2}$ Rydberg state at the interaction time $t = 4$ μs and scanning of the third-stage laser frequency detuning from the single-photon resonance. The spectrum S (Fig. 2a) corresponds to the average number of Rydberg atoms detected per laser pulse. Spectra S_1-S_5 (Figs 2b–2f) represent the excitation spectra of mesoscopic ensembles with the number of Rydberg atoms $N = 1-5$, respectively. The sum of these spectra gives the total measurable spectrum S. Similar spectra for the $37P_{3/2}$ Rydberg state were discussed in detail in our paper [13].

A three-photon resonance arises at a detuning $\delta_3 \approx -162$ MHz, which is a consequence of the total detuning of laser frequencies $\delta_1 + \delta_2 = +162$ MHz from two intermediate resonances. Such a resonance corresponds to coherent three-photon excitation without noticeable population of the intermediate levels $5P_{3/2}$ and $6S_{1/2}$ [12], which is accompanied by the absorption of all three photons simultaneously. Therefore, Rabi oscillations are observable in this case. The measured width 2.3 MHz of the spectrum S in Fig. 2a is due to the following factors: the sum of the linewidths of the three lasers, $(\Gamma_1 + \Gamma_2 + \Gamma_3)/(2\pi) \approx 0.6$ MHz; the dynamic field broadening $\Omega/(2\pi) \approx 0.2$ MHz; the Fourier widths of the exciting laser pulses assumed to be the same and equal to $1/t \approx 0.25$ MHz; the additional Zeeman broadening $\Gamma_Z/(2\pi) \approx 0.2$ MHz, and the additional radiative broadening due to the nonzero probability of population of intermediate short-lived levels of the three-photon transition. The latter depends on many parameters and cannot be easily estimated; therefore, to compare the experimental spectrum S in Fig. 2a with the theoretical one, we used a numerical calculation.

The solid thick curve in Fig. 2a shows the results of numerical calculations using our four-level model [12]. The fitting parameters were the single-photon Rabi frequencies and the average number of atoms in the laser excitation volume. According to experimental data, the single-photon Rabi frequencies were: $\Omega_1/(2\pi) \approx 6$ MHz, $\Omega_2/(2\pi) \approx 220$ MHz и $\Omega_3/(2\pi) \approx 2$ MHz. The best agreement with experiment was obtained at practically the same values: $\Omega_1/(2\pi) = 6$ MHz, $\Omega_2/(2\pi) = 220$ MHz и $\Omega_3/(2\pi) = 2$ MHz. In the calculation, we used the three-photon Rabi frequency $\Omega/(2\pi) = 0.2$ MHz, the average number of cold atoms $N_0 = 10$, and the probability of detecting Rydberg atoms $T = 0.6$.

We performed the analysis of the excitation spectra of mesoscopic ensembles of N Rydberg atoms earlier in Ref. [13] for noninteracting atoms in the $37P_{3/2}$ state and in Ref. [14] for atoms in the $39P_{3/2}$, $81P_{3/2}$, and $110P_{3/2}$ states. For the last two states, a partial dipole blockade was observed due to the interactions of the Rydberg atoms. Let us briefly recall the features of the measured 'polyatomic' spectra. In the absence of interatomic interactions, which is characteristic of the $39P_{3/2}$ state studied in the present work and the S_N spectra in Figs 2b–2f, these spectra are described by the statistics of excitation and detection of Rydberg atoms [14].

Let a mesoscopic ensemble of N_0 Rb atoms in the ground state be in the excitation volume prior to the onset of the laser pulse. During the laser pulse, there is a nonzero probability p ($0 \leqslant p \leqslant 1$) of excitation of each of the atoms to the Rydberg state. The probability p depends on the three-photon detun-

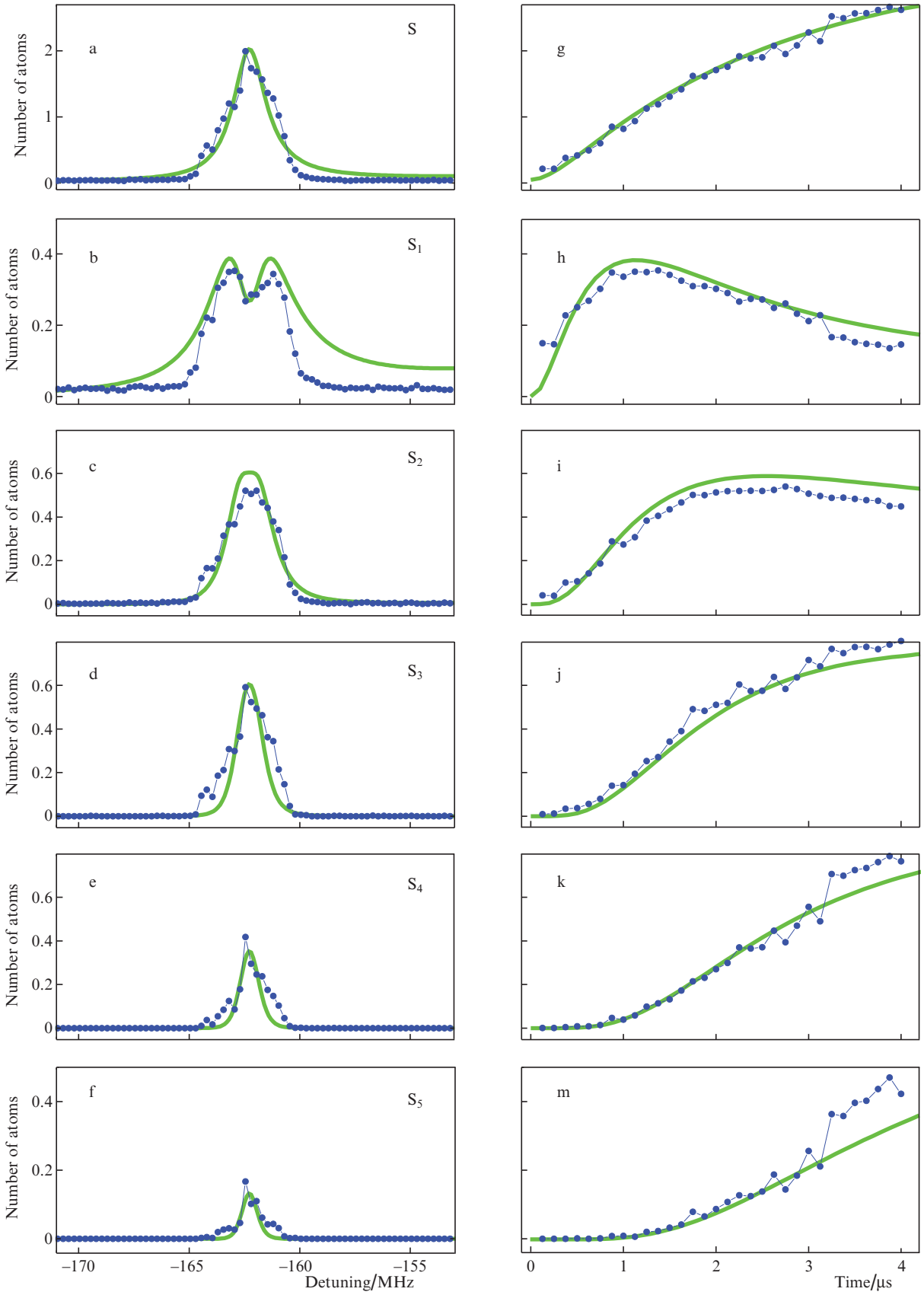

Figure 2. (Colour online) (a–f) Experimental (points) spectra of three-photon laser excitation of the $39P_{3/2}$ Rydberg state for the interaction time of $t = 4$ μs and the detuning δ_3 of the third-stage laser being scanned; the spectrum S corresponds to the average number of Rydberg atoms detected per laser pulse, the spectra $S_1 - S_5$ are the excitation spectra of mesoscopic ensembles with the number of Rydberg atoms $N = 1-5$, respectively, their sum giving the total measurable spectrum S. Solid curves are the result of numerical simulation for the three-photon Rabi frequency $\Omega/(2\pi) = 0.2$ MHz, the average number of atoms $N_0 = 10$, and the probability of their detection $T = 0.6$. (g–m) Amplitudes of resonances in the spectra (a–e) at the centres of the transition lines versus the excitation time at $N_0 = 13$.

ing and, under certain conditions, is given by Eqn (1) or Eqn (2). Then the average number of Rydberg atoms excited per laser pulse is

$$\bar{n} = pN_0. \tag{3}$$

The statistics of the number of Rydberg atoms excited per laser pulse is described by the probability of finding N Rydberg atoms after a single laser pulse according to the normal distribution

$$P_N = p^N (1-p)^{N_0-N} \frac{N_0!}{N!(N_0-N)!}, \tag{4}$$

which is valid for any p and N_0. Such a statistical distribution would be observed for an ideal detector of Rydberg atoms, which has a detection probability $T = 1$. For real detectors, the detection probability is always less than unity. For example, in our experiment [17], it was about 0.7, which is record-breaking for Rydberg atoms. It can be easily shown that, taking into account the finite detection probability, we will have the following distribution for the probability of recording N Rydberg atoms:

$$\tilde{P}_N = (pT)^N (1-pT)^{N_0-N} \frac{N_0!}{N!(N_0-N)!}. \tag{5}$$

As a result, the average number of Rydberg atoms detected per laser pulse decreases to $\bar{n}T$. It is this quantity that is measured experimentally by averaging over a large number of laser pulses.

The total signal corresponding to the average number of atoms detected per laser pulse and the corresponding spectrum S in Fig. 2a are expressed as

$$\mathrm{S} = pN_0 T = \sum_{N=1}^{N_0} N\tilde{P}_N = \sum_{N=1}^{N_0} \mathrm{S}_N. \tag{6}$$

In this case, for the spectral dependence of the excitation probability, one should set $p = \rho_{33}$, i.e., the total spectrum S is in fact the result of averaging over a different number of registered atoms N. The solution of the inverse problem yields the following formula for the 'polyatomic' spectra S_N in Figs 2b–2f:

$$\mathrm{S}_N = N(pT)^N (1-pT)^{N_0-N} \frac{N_0!}{N!(N_0-N)!}. \tag{7}$$

Then the 'polyatomic' spectra for the previously determined parameter $N_0 = 10$ and $T = 0.6$ are given by the expressions

$$\mathrm{S}_1 = (\rho_{33}T)^1(1-\rho_{33}T)^9 10,$$

$$\mathrm{S}_2 = (\rho_{33}T)^2(1-\rho_{33}T)^8 90,$$

$$\mathrm{S}_3 = (\rho_{33}T)^3(1-\rho_{33}T)^7 360, \tag{8}$$

$$\mathrm{S}_4 = (\rho_{33}T)^4(1-\rho_{33}T)^6 840,$$

$$\mathrm{S}_5 = (\rho_{33}T)^5(1-\rho_{33}T)^5 1260.$$

For mesoscopic ensembles with a small number N_0 of atoms, under a sufficiently strong excitation a dip can form at the centre of a polyatomic resonance due to a purely statistical effect: the probability of excitation and detection of more than one atom exceeds the probability of excitation and registration of only one atom.

It is exactly this effect that is observed in Fig. 2b, namely, a dip in the centre of the single-atom spectrum S_1. For two atoms, there is no dip in the S_2 spectrum, but there is a flat top, which is also due to a decrease in the probability of excitation of two atoms at the resonance centre. For a larger number of atoms, there is no dip in polyatomic spectra. The amplitudes of polyatomic spectra decrease with increasing N. For their theoretical description, the calculated spectrum $\mathrm{S} = \rho_{33}N_0T$ (Fig. 2a) was substituted into Eqns (8). As can be seen from Figs 2b–2f, there is good agreement between experiment (dots) and theory (solid curves) for the amplitudes and shapes of all polyatomic spectra S_N. Small discrepancies at their wings are a consequence of the features of the theoretical model of phase diffusion when the finite radiation linewidths of three lasers are taken into account. As our previous experiment [14] showed, agreement between experiment and theory can only be violated for interacting Rydberg atoms under dipole blockade conditions; therefore, polyatomic spectra can be used to study it.

Let us now turn to the analysis of the temporal dynamics of the excitation of mesoscopic ensembles of Rydberg atoms, which is the main goal of this work. The dots in Figs 2g–2m show the experimental dependences of the amplitudes of the multiatomic three-photon spectra at the centre of the laser excitation line of the $39P_{3/2}$ Rydberg state on the interaction time t. As in Figs 2a–2f, the curve in Fig. 2g corresponds to the average number of Rydberg atoms detected per laser pulse, and the curves in Figs 2h–2l correspond to the dynamics of excitation of mesoscopic ensembles with the number of Rydberg atoms $N = 1$–5, respectively.

Since it has already been determined for Fig. 2 that the three-photon Rabi frequency $\Omega/(2\pi) = 0.2$ MHz, and the observed width of spectrum S equal to 2.3 MHz is much larger, Eqn (2) can be considered applicable for theoretical analysis. For the amplitude of the spectrum at $\delta = 0$, we obtain:

$$\rho_{33}(\delta = 0) \approx \frac{\Omega^2}{2\Omega^2 + \gamma^2}\left[1 + \mathrm{e}^{-\gamma t} - 2\mathrm{e}^{-\gamma t/2}\cos(\Omega t)\right]. \tag{9}$$

Since $\Omega \ll \gamma$, at $t \to 0$ Eqn (9) yields a quadratic dependence on time, $\rho_{33} \approx \gamma^2 t^2/4$. At $t \to \infty$, the population in Eqn (9) approaches a stationary value $\rho_{33} \approx \Omega^2/\gamma^2$. For intermediate t, the growing dependence will be observed having the form of a saturation curve. Because of small Ω, there are no Rabi oscillations. Formula (9) is approximate; therefore, in a general case of comparing theory and experiment, a numerical calculation within the four-level model should be used.

The solid curve in Fig. 2g shows the result of numerical calculation of the dynamics of the spectrum $\mathrm{S} = \rho_{33}N_0T$ at $\Omega/(2\pi) = 0.2$ MHz. The best agreement with experiment was achieved with fitting parameters $N_0 = 13$ and $T = 0.6$. Using these parameters and formula (7), we can calculate the temporal dynamics of the polyatomic spectra S_1–S_5:

$$\tilde{\mathrm{S}}_1 = (\rho_{33}T)^1(1-\rho_{33}T)^{12} 13,$$

$$\tilde{S}_2 = (\rho_{33}T)^2(1-\rho_{33}T)^{11}156,$$

$$\tilde{S}_3 = (\rho_{33}T)^3(1-\rho_{33}T)^{10}858, \quad (10)$$

$$\tilde{S}_4 = (\rho_{33}T)^4(1-\rho_{33}T)^{9}2680,$$

$$\tilde{S}_5 = (\rho_{33}T)^5(1-\rho_{33}T)^{8}6435.$$

The solid curves in Figs 2h–2m show the results of numerical calculations for the dynamics of polyatomic spectra S_1–S_5. The single-atom signal in Fig. 2h first increases (up to $t = 1$ μs), and then begins to decrease, since the probability of excitation of more than one atom begins to increase. The diatomic signal in Fig. 2i appears with some delay relative to the signal in Fig. 2h and is close to zero up to $t = 0.25$ μs, then it first increases (up to $t = 2$ μs), after which it also begins to decrease. For other polyatomic signals, there is an increasing delay in their appearance with a subsequent increase in signals. Good agreement between theory and experiment for all signals indicates both the adequacy of the four-level model and the correctness of the statistical analysis of the probabilities of polyatomic excitation of mesoscopic ensembles of Rydberg atoms. In this case, by fitting the theory to experiment, it is possible to determine unknown experimental parameters, such as the three-photon Rabi frequency, the average number of atoms in the volume of laser excitation, and the probability of their detection.

To study the possibility of observing Rabi oscillations upon three-photon laser excitation to the Rydberg states of mesoscopic ensembles of atoms, we measured the spectra and dynamics for a higher three-photon Rabi frequency. The powers of the lasers used at all stages of excitation were increased by several times, and the concentration of atoms in the trap was reduced to avoid saturation of the VEU-6 signals. According to the results of experimental measurements, single-photon Rabi frequencies were: $\Omega_1/(2\pi) \approx 10$ MHz, $\Omega_2/(2\pi) \approx 500$ MHz and $\Omega_3/(2\pi) \approx 6$ MHz.

The dots in Fig. 3 show the experimental spectra and dynamics of the three-photon laser excitation of the $39P_{3/2}$ Rydberg state, similar to those shown in Fig. 2. Solid lines show the results of numerical calculations. Both for the spectra and for their dynamics, the best agreement between experiment and theory was obtained at $\Omega_1/(2\pi) = 10$ MHz, $\Omega_2/(2\pi) = 500$ MHz and $\Omega_3/(2\pi) = 14$ MHz. In this case, when calculating the three-photon Rabi frequency $\Omega/(2\pi) = 0.36$ MHz, the average number of atoms was $N_0 = 5$, and the probability of detecting Rydberg atoms was $T = 0.6$. The theory was compared with experiment using Eqns (6) and (7).

The polyatomic spectra in Figs 3a–3f are basically similar to those in Figs 2a–2f, except that the spectra S_3–S_5 have lower amplitudes due to the smaller average number of excited atoms. The widths of the spectra practically did not change, despite the increase in the Rabi frequency. This suggests that the main source of their broadening is the laser linewidth and the additional Zeeman broadening. Experimental polyatomic spectra are described by theory well.

However, the temporal dynamics in Figs 3g–3m is seen to change significantly. The signal in Fig. 3g saturates at $t = 1$ μs. Up to this time, there is a noticeable discrepancy between experiment and theory: the theory predicts a quadratic dependence on time at $t \to 0$, followed by a linear increase and saturation, while in the experiment a linear increase is observed immediately. This becomes even more noticeable for the signals in Figs 3h–3i. For the signals in Figs 3j–3m, the agreement with the theory becomes better. Also noteworthy are the signatures of the first Rabi oscillation in the S_1 signal in Fig. 3h, but with a rather low contrast. This is because the three-photon Rabi frequency is smaller than the width of the three-photon spectrum, which corresponds to a coherence time of ~1 μs.

The physical nature of the discrepancy between theory and experiment at short times in the dynamics of the total spectrum S and for the spectra S_1 and S_2 is not yet clear. The theory predicts a quadratic growth of the signal with increasing time according to Eqn (9). This is due to the presence of some coherence of the laser excitation at short times, when the dephasing of atomic states has not yet occurred due to parasitic broadening of the three-photon resonance.

However, in the experiment for these signals, an increase close to linear is observed. This behaviour could be simulated by significantly increasing parasitic broadenings, but in this case, the width of the three-photon spectrum would inevitably increase, which is not observed in practice. The introduction of the residual Doppler broadening into the theoretical model due to the finite temperature of the atoms (~100 μK) and inhomogeneity of the radiation intensities at the intersection of the second and third stage laser beams in the laser excitation volume did not lead to a linear growth of the signals. We also note that in a similar experimental work [19] for a large atomic ensemble, the use of a rectangular intensity distribution did not significantly improve the contrast of Rabi oscillations, and only the beginning of the first oscillation was observed.

To search for possible ways to observe Rabi oscillations, we performed extended theoretical calculations. Figure 4 shows the results of a numerical calculation of the Rabi oscillations of the population ρ_{33} of the $39P_{3/2}$ Rydberg state of the Rb atom as a result of three-photon excitation at a three-photon Rabi frequency $\Omega/(2\pi) = 360$ kHz and various parameters of parasitic broadening, damping the Rabi oscillations. The curve in Fig. 4a corresponds to the theoretical curve in Fig. 3g with the following parameters: laser linewidths $\Gamma_1/(2\pi) = \Gamma_2/(2\pi) = 300$ kHz и $\Gamma_3/(2\pi) = 10$ kHz; Zeeman broadening $\Gamma_Z/(2\pi) = 100$ kHz; and the radiative width of the Rydberg state $\gamma_R/(2\pi) = 3{,}2$ kHz. With these parameters, only the beginning of the first oscillation with low contrast is observed.

As the linewidths of all lasers decrease to 10 kHz (Fig. 4b), the contrast of the first oscillation increases and the second and third oscillations appear, which indicates the importance of narrowing the laser lines. Further, when the Zeeman broadening is eliminated ($\Gamma_Z = 0$, Fig. 4c), the contrast of Rabi oscillations increases significantly. This means that the quadrupole magnetic field of the magneto-optical trap must be turned off before excitation of atoms to the Rydberg state. This turnoff usually takes at least 1 ms due to the inductances of the magnetic field coils and parasitic Foucault currents on the walls of the vacuum chamber. Accordingly, the repetition rate of laser pulses will have to be reduced to less than 1 kHz, which will significantly increase the measurement time and the requirements for the long-term stability of the radiation frequencies of all lasers. With a further decrease in the linewidths of all lasers to 1 kHz (Fig. 4d), the oscillation contrast also noticeably increases.

Thus, to observe Rabi oscillations reliably in our experiments on three-photon laser excitation of Rydberg atoms, it is necessary to turn off the quadrupole magnetic field, and for

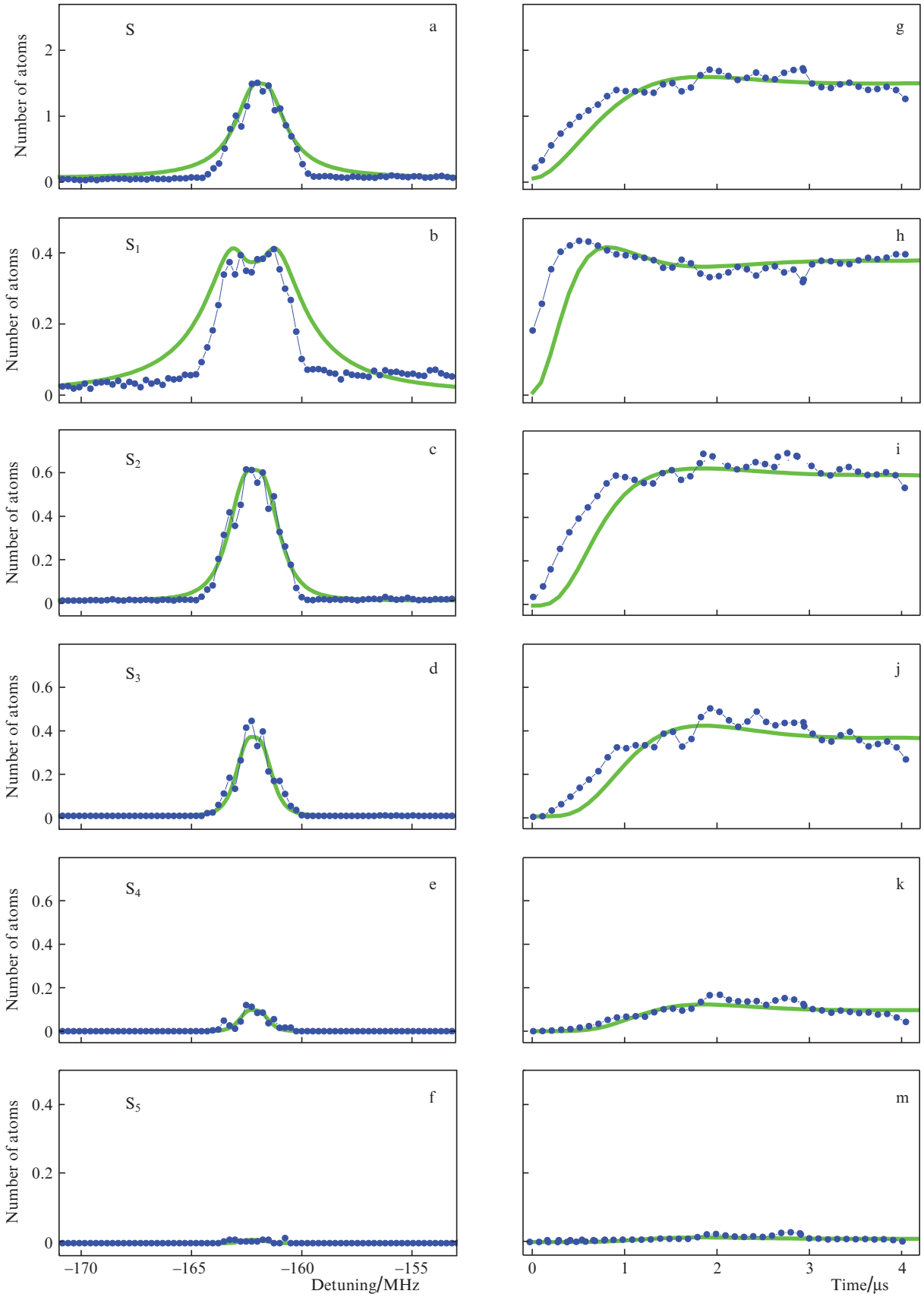

Figure 3. (Colour online) (a–f) Experimental (points) spectra of three-photon laser excitation of the $39P_{3/2}$ Rydberg state for the interaction time of $t = 4$ μs and the detuning δ_3 of the third-stage laser being scanned; the spectrum S corresponds to the average number of Rydberg atoms detected per laser pulse, the spectra $S_1 - S_5$ are the excitation spectra of mesoscopic ensembles with the number of Rydberg atoms $N = 1-5$, respectively, their sum giving the total measurable spectrum S. Solid curves are the result of numerical simulation for the three-photon Rabi frequency $\Omega/(2\pi) = 0.36$ MHz, the average number of atoms $N_0 = 5$, and the probability of their detection $T = 0.6$. (g–m) Amplitudes of resonances in the spectra (a–e) at the centres of the transition lines versus the interaction time.

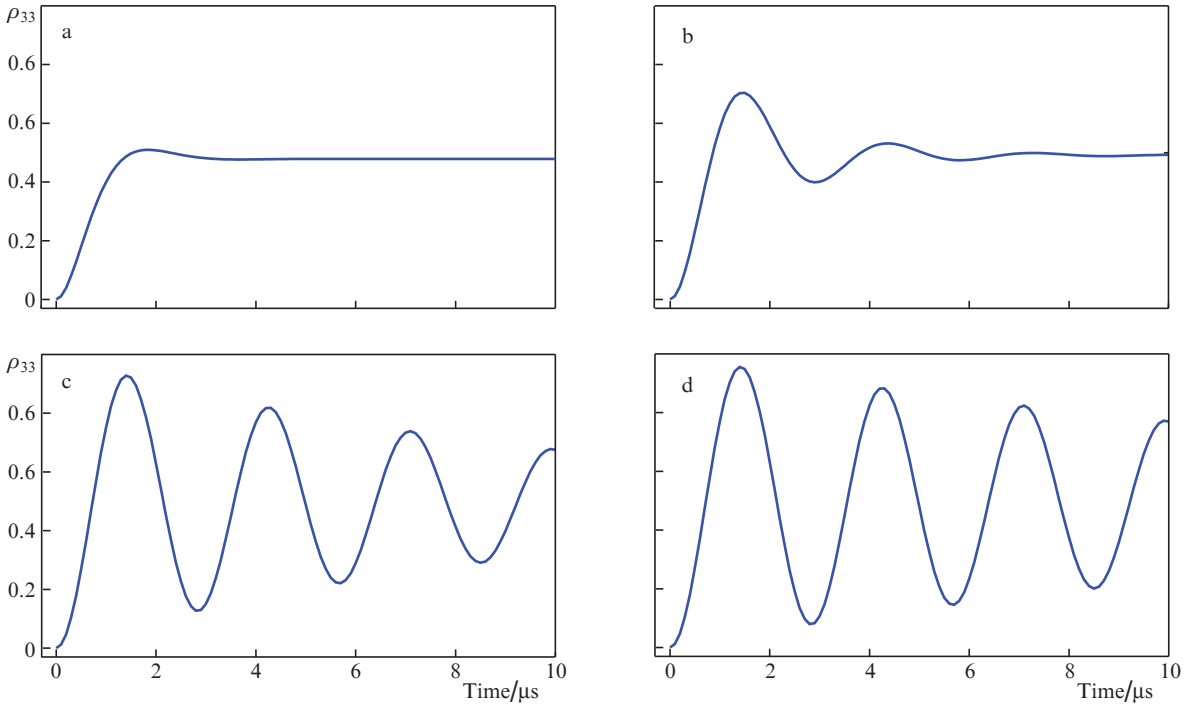

Figure 4. Numerical calculation of the Rabi oscillations of the population ρ_{33} of the $39P_{3/2}$ Rydberg state of the Rb atom as a result of three-photon excitation at $\Omega/(2\pi) = 360$ kHz and various parasitic broadening parameters: (a) $\Gamma_1/(2\pi) = \Gamma_2/(2\pi) = 300$ kHz, $\Gamma_3/(2\pi) = 10$ kHz, $\Gamma_Z/(2\pi) = 100$ kHz; (b) $\Gamma_1/(2\pi) = \Gamma_2/(2\pi) = \Gamma_3/(2\pi) = 10$ kHz, $\Gamma_Z/(2\pi) = 100$ kHz; (c) $\Gamma_1/(2\pi) = \Gamma_2/(2\pi) = \Gamma_3/(2\pi) = 10$ kHz, $\Gamma_Z/(2\pi) = 0$; and (d) $\Gamma_1/(2\pi) = \Gamma_2/(2\pi) = \Gamma_3/(2\pi) = 1$ kHz, $\Gamma_Z/(2\pi) = 0$.

all lasers to ensure line widths and their frequency stability no worse than 10 kHz. This is a technically difficult but feasible task [3].

At the same time, even in Fig. 4d, the Rabi oscillations do not reach the maximum contrast and decay with a time constant of about 15 μs, while the effective radiative lifetime of the $39P_{3/2}$ Rydberg state in Rb atoms is about 50 μs at a temperature of 300 K [20]. This indicates an additional damping of coherence upon three-photon excitation. Preliminary theoretical analysis and numerical calculations showed that it is due to the presence of some population of the intermediate states of the three-photon transition at the existing frequency detunings of laser radiation from intermediate resonances. The method of fighting this phenomenon should be to increase detunings by an order of magnitude or more. For applications in quantum information, it is also planned to use atoms in higher Rydberg states ($n \sim 100$) with much longer radiative lifetimes (~500 μs), which should further reduce the loss of coherence upon three-photon excitation. These studies will be the subject of our future work.

5. Conclusions

This paper is devoted to the experimental and theoretical study of the dynamics of three-photon $5S_{1/2} \rightarrow 5P_{3/2} \rightarrow 6S_{1/2} \rightarrow 39P_{3/2}$ laser excitation of mesoscopic ensembles of cold Rb atoms to Rydberg states in a magneto-optical trap using cw single-frequency lasers at each stage. Ensembles of Rydberg atoms consisted of $N = 1-5$ atoms and were detected by the method of selective field ionisation with postselection by the number of atoms. The dependences of the excitation probability on the duration of the exciting laser pulses and the number of registered Rydberg atoms were studied.

In experiments, a linear increase in probabilities was observed at short interaction times, and at large times the probabilities reached saturation, each number of atoms having its own features. The experimental dependences were compared with the results of numerical calculations in the framework of a four-level model with a density matrix that takes into account various parasitic broadenings of resonances. At short times, the theory predicts a quadratic increase in the probability signal and there is some discrepancy with experiment, while at long times, they are in good agreement.

Using numerical simulation, we also determined the conditions necessary to observe Rabi oscillations of the populations in our experiments: the quadrupole magnetic field of the magneto-optical trap should be turned off to eliminate Zeeman broadening, and for all lasers, line widths and their frequency stability should be no worse than 10 kHz. The results obtained are important for the application of Rydberg atoms in quantum information.

References

1. Saffman M., Walker T.G., Mølmer K. *Rev. Mod. Phys.*, **82**, 2313 (2010).
2. Ryabtsev I.I., Beterov I.I., Tretyakov D.B., Entin V.M., Yakshina E.A. *Phys. Usp.*, **59**, 196 (2016) [*Usp. Fiz. Nauk*, **182**, 206 (2016)].
3. Saffman M. *J. Phys. B*, **49**, 202001 (2016).
4. Gallagher T.F. *Rydberg Atoms* (Cambridge: Cambridge University Press, 1994).
5. Lukin M.D., Fleischhauer M., Cote R., Duan L.M., Jaksch D., Cirac J.I., Zoller P. *Phys. Rev. Lett.*, **87**, 037901 (2001).
6. Comparat D., Pillet P. *J. Opt. Soc. Am. B*, **27**, A208 (2010).
7. Henriet L., Beguin L., Signoles A., Lahaye T., Browaeys A., Reymond G.-O., Jurczak C. *Quantum*, **4**, 327 (2020).
8. Cubel T., Teo B.K., Malinovsky V.S., Guest J.R., Reinhard A., Knuffman B., Berman P.R., Raithel G. *Phys. Rev. A*, **72**, 023405 (2005).

9. Reetz-Lamour M., Deiglmayr J., Amthor T., Weidemüller M. *New J. Phys.*, **10**, 045026 (2008).
10. Sautenkov V.A., Saakyan S.A., Bobrov A.A., Vilshanskaya E.V., Zelener B.B., Zelener B.V. *J. Opt. Soc. Am. B*, **35**, 1546 (2018).
11. Ryabtsev I.I., Beterov I.I., Tretyakov D.B., Entin V.M., Yakshina E.A. *Phys. Rev. A*, **84**, 053409 (2011).
12. Entin V.M., Yakshina E.A., Tretyakov D.B., Beterov I.I., Ryabtsev I.I. *J. Exp. Theor. Phys.*, **116**, 721 (2013) [*Zh. Eksp. Teor. Fiz.*, **143** (5), 831 (2013)].
13. Yakshina E.A., Tretyakov D.B., Entin V.M., Beterov I.I., Ryabtsev I.I. *Quantum Electron.*, **48** (10), 886 (2018) [*Kvantovaya Elektron.*, **48** (10), 886 (2018)].
14. Yakshina E.A., Tretyakov D.B., Entin V.M., Beterov I.I., Ryabtsev I.I. *J. Exp. Theor. Phys.*, **130** (2), 170 (2020) [*Zh. Eksp. Teor. Fiz.*, **157** (2), 206 (2020)].
15. Tretyakov D.B., Beterov I.I., Entin V.M., Ryabtsev I.I., Chapovsky P.L. *J. Exp. Theor. Phys.*, **108**, 374 (2009) [*Zh. Eksp. Teor. Fiz.*, **135**, 428 (2009)].
16. Ryabtsev I.I., Tretyakov D.B., Beterov I.I., Entin V.M. *Phys. Rev. A*, **76**, 012722 (2007); Erratum: *Phys. Rev. A*, **76**, 049902 (E) (2007).
17. Tretyakov D.B., Beterov I.I., Yakshina E.A., Entin V.M., Ryabtsev I.I., Cheinet P., Pillet P. *Phys. Rev. Lett.*, **119**, 173402 (2017).
18. Agarwal G.S. *Phys. Rev. Lett.*, **37**, 1383 (1976).
19. Reetz-Lamour M., Amthor T., Deiglmayr J., Weidemüller M. *Phys. Rev. Lett.*, **100**, 253001 (2008).
20. Beterov I.I., Ryabtsev I.I., Tretyakov D.B., Entin V.M. *Phys. Rev. A*, **79**, 052504 (2009).